He atom near methane-plated MgO: Interaction and scattering

David R. Jung, Jinhe Cui, Daniel R. Frankl, G. Ihm, H.-Y. Kim, and M. W. Cole
Department of Physics, The Pennsylvania State University, University Park, Pennsylvania 16802
(Received 21 June 1989)

Scattering experiments and potential-energy calculations are reported for the system consisting of a He atom near a MgO surface upon which is adsorbed a CH_4 layer. Assuming either a fixed dipolar configuration or free rotation of the molecule, the theoretical potential yields bound-state–resonance (selective-adsorption) positions consistent with those measured experimentally.

I. INTRODUCTION

Interest has grown recently[1–8] in the subject of inert-gas adsorption on the MgO(001) surface. A major stimulus is the fact that this surface presents a quite different symmetry (square) from that of the much-studied graphite basal plane. This leads to new kinds of energy competition between alternative adsorbate structures. In particular, the close-packed overlayer structure is usually less favored on MgO than on graphite. Experimental access to this problem was first achieved when it was realized that oxidized Mg particles ("smoke") provide homogeneous substrates of high specific surface area.[1] The latter is not a requirement, of course, for single surface probes such as electron and atom scattering.

One of the techniques recently applied to study adsorbed films is helium-atom scattering. This has the ability to provide quite precise information about both the film (structure and dynamics) and the interaction of the He atom with the film-substrate system.[9–16] The latter is a sensitive test of our models of many-body interactions.[17]

The present study is directed to the case of CH_4 adsorption on MgO. This system has been studied previously by thermodynamic methods,[18] and by electron[3] and neutron scattering.[5] The CH_4 layer forms a $c(2\times2)$ commensurate solid at low temperature, due in part to the compatibility between the lattice constant of MgO (4.21 Å) and the intermolecular spacing in the CH_4 three-dimensional solid (4.18 Å).

The outline of this paper is as follows. Section II describes calculations of the He adsorption potential for the case of a commensurate layer. Four different assumptions about the rotational configuration are considered: free rotor, tripod, and dipod orientations. Section III describes the experimental procedures and results. Section IV compares the measured bound-state–resonance energies with the calculated values. Fair agreement with the data for temperatures from 22 to 46 K is found for the free rotor and dipod cases, while the tripod calculation disagrees with experiment. Section V summarizes our results.

II. CALCULATION OF THE POTENTIAL AND SPECTRUM

We write the He potential energy $V(\mathbf{r})$ in a two-dimensional Fourier series based on a $c(2\times2)$ commensurate structure of the CH_4 monolayer,

$$V(\mathbf{r})=V_0(z)+\sum_{\mathbf{G}} V_{\mathbf{G}}(z)e^{i\mathbf{G}\cdot\mathbf{R}} \tag{1}$$

where $\mathbf{R}(x,y)$ and z are, respectively, the coordinates of the He atom parallel and perpendicular to the surface, with the origin located at a carbon nucleus. $V_0(z)$ is the laterally averaged potential and the periodic terms have Fourier components $V_{\mathbf{G}}(z)$. For the $c(2\times2)$ superlattice, the square unit cell has side length $a=4.21$ Å and a lowest-order reciprocal lattice vector of length $|\mathbf{G}_{10}|=1.49$ Å^{-1}. The interaction can also be written[14] as a sum of terms,

$$V(\mathbf{r})=V_a(\mathbf{r})+V_s(z)+V_3^{a\text{-}a}(z)+V_3^{a\text{-}s}(z)+V_t(\mathbf{r}) . \tag{2}$$

The first term $V_a(\mathbf{r})$ represents the interaction between a He atom and the CH_4 monolayer, considering only two-body interactions. In general, $V_a(\mathbf{r})$ depends on the molecular orientations $\mathbf{\Omega}_i$ due to the anisotropy of the CH_4 molecule,

$$V_a(\mathbf{r})=\sum_i U(\mathbf{r},\mathbf{R}_i,\mathbf{\Omega}_i) , \tag{3}$$

where the sum is over the CH_4 lattice sites $\mathbf{R}_i$ and U is the He-CH_4 pairwise interaction. The form adopted here is the Hartree-Fock-dispersion (HFD) potential given by Buck *et al.*[19] which is expanded in a series involving spherical harmonics Y_{lm} that reflect the tetrahedral symmetry of methane:

$$\begin{aligned} &U(\rho,\gamma,\phi)=U_0(\rho)+U_3(\rho)T_3(\gamma,\phi)+U_4(\rho)T_4(\gamma,\phi) ,\\ &T_3(\gamma,\phi)=i[Y_{32}(\gamma,\phi)-Y_{3-2}(\gamma,\phi)] ,\\ &T_4(\gamma,\phi)=\sqrt{5}Y_{44}(\gamma,\phi)+\sqrt{14}Y_{40}(\gamma,\phi)\\ &\qquad\qquad +\sqrt{5}Y_{4-4}(\gamma,\phi) . \end{aligned} \tag{4}$$

Here ρ is the distance between the atom and the center of mass of the molecule and γ and ϕ are the corresponding spherical angular coordinates.[20] $U_0(\rho)$ represents the isotropic part of the potential. Explicit expressions for $U_i(\rho)$ are given in Ref. 19.

The second term in Eq. (2) represents the He-MgO potential. Based on the asymptotic form we write this as a sum of contributions from individual layers,

$$V_s=-\frac{3C_3}{d^3}\sum_i^{\infty}\left[j+\frac{z+z_a}{d}\right]^{-4} . \tag{5}$$

Here $C_3=151$ meV is the asymptotic dispersion coefficient[21] and $d=2.103$ Å is the spacing between consecutive layers of the MgO crystal. $z_a=3$ Å is the distance of the methane layer from the top plane of the MgO nuclei.[22] Since the atom is at relatively large distance (≈ 6.4 Å) from the substrate surface, V_s can be approximated as

$$V_s\approx-\frac{C_3}{(z+b)^3} , \tag{6}$$

with $b=2.076$ Å, determined by equating Eq. (5) to Eq.(6) at $z=3.4$ Å. We believe that the V_s term is the major source of theoretical uncertainty [through both C_3 (Ref. 21) and z_a (Ref. 22) values]; an estimate would be $\pm 20\%$, i.e., ≈ 0.3 meV at the total potential minimum.

$V^{a\text{-}a}(z)$ and $V^{a\text{-}s}(z)$ are contributions to Eq. (2) representing the leading many-body corrections to the previous two potentials. $V^{a\text{-}a}(z)$ is obtained by summing the three-body Axilrod-Teller-Muto[23] triple-dipole interactions between the He atom and all possible pairs of CH_4 atoms in the monolayer. Our result for the lateral average is well described by

$$V_3^{a\text{-}a}=(\nu/a^9)\Gamma_0(z/a) . \tag{7}$$

Here $\nu=13.8$ eV Å^9 (Ref. 24) for the case of He above a CH^4 layer, $a=4.21$ Å, and

$$\Gamma_0(x)\approx 112\exp(-3.78x) \tag{8}$$

in the distance regime of interest here ($x\approx 0.75$). This result is essentially identical to that of Klein and Cole[25] for a noble gas atom near a triangular lattice layer having the same density of atoms. We neglected the Fourier components of this three-body term because they are negligible; the largest coefficient value at the potential minimum is $\approx 3\times 10^{-3}$ meV.

$V^{a\text{-}s}(z)$ is the MgO substrate-mediated interaction with the adlayer. Its contribution to the lateral average potential of the He is given by[26]

$$V_3^{a\text{-}s}=-\frac{\pi n}{2}\frac{C_{s2}}{(z+2b)^4} , \tag{9}$$

where $n=0.056$ Å^{-2} is the areal density of CH_4. The strength coefficient C_{s2} can be calculated from[24]

$$C_{s2}=\frac{3}{\pi}\int_0^{\infty}dE\,\alpha_{He}(iE)\alpha_{CH_4}(iE)[g(iE)]^2 , \tag{10}$$

where

$$g(iE)\equiv\frac{\epsilon(iE)-1}{\epsilon(iE)+1}\approx g_0[1+(E/E_s)^2]^{-1} . \tag{11}$$

$\alpha(iE)$ is the dynamical polarizability of the molecule or He atom and $\epsilon(iE)$ is the dielectric function of the MgO substrate. C_{s2} is evaluated as 1.39 eV Å^{-6} using $E_s=20.4$ eV, $g_0=0.53$,[27] and other parameters in Rauber *et al.*[24]

The last term $V_t(\mathbf{r})$ is the effect of thermal vibrations of the adlayer. It can be evaluated by assuming that the probability density of the adlayer is Gaussian distributed in the z direction (as is valid in the present case of small vibrations),[28]

$$V_t(\mathbf{r})\cong\frac{\langle z_\alpha^2\rangle}{2}\sum_{\mathbf{G}}\frac{d^2V_{a\mathbf{G}}(z)}{dz^2}e^{i\mathbf{G}\cdot\mathbf{R}}\cong\frac{\langle z_a^2\rangle}{2}\frac{d^2V_a}{dz^2} , \tag{12}$$

$$\langle z_\alpha^2\rangle=\frac{\hbar}{2m_a\omega_a}\coth\left[\frac{\hbar\omega_a}{2k_BT}\right] , \tag{13}$$

where the effective frequency ω_a reflects forces due to both the adlayer and the substrate. We derive $\hbar\omega_a\approx 12$ meV (except for the tripod configuration, in which case it is ≈ 10 meV) from the work of Girard and Girardet.[8] The magnitude of V_t (for the laterally averaged free-rotor case) is ≈ 0.1 meV near the minimum of V in the temperature regime $22<T<46$ K relevant to the experiment.[28]

In our model, the orientational dependence of $V(\mathbf{r})$ mainly arises from the term V_a.[29] We have considered four different configurations: (i) free-rotor, (ii) dipod (010), (iii) dipod (011), and (iv) parallel (010) tripods with C atoms above the Mg ions. $V_0(z)$ for each configuration is presented in Fig. 1. A recent calculation by Deprick and Julg[7] showed that an isolated molecule should have

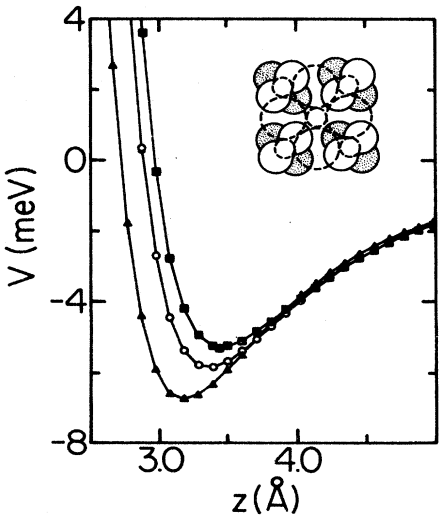

FIG. 1. Laterally averaged potentials $V_0(z)$ corresponding to four different CH_4 configurations are presented: (i) free rotor (solid squares), (ii) dipod (010) and (iii) dipod (011) (circles), and (iv) tripod (solid triangles). The inset shows the dipod (011) configuration [as discussed in Ref. (7)] in which the tetrahedral CH_4 molecules (composed of solid circles) are located above Mg ions (small dashed circles) and oriented along the (011) direction of the bulk MgO unit cell.

the dipod (010) orientation, but that a monolayer could equally well have the (011) orientation. In contrast, the results of Girard and Girardet[8] show that the tripod configuration is slightly favored for an isolated molecule. We will discuss in Sec. IV whether He scattering can distinguish between these various possibilities. We have tested the sensitivity of the interaction potential to the model of the interatomic potential U. The use of an isotropic Lennard-Jones (LJ) He-CH_4 pair potential with parameters $\epsilon=2.2$ meV and $\sigma=3.421$ Å (which are chosen to reproduce the experimentally determined equilibrium position and well depth[19]) gives a steeper repulsion and a deeper well (by ≈ 0.8 meV) for the monolayer problem. Thus one has to use the accurate potential form in order to have any chance of getting reliable results.

For the free-rotor configuration, the Fourier components depend only on the magnitude of the reciprocal lattice vectors $|\mathbf{G}_{ij}|=(i^2+j^2)^{1/2}|\mathbf{G}_{10}|$. The contribution of the adlayer term is[30]

$$V_{aG}(z)=2\pi n\int_0^\infty J_0(Gt)U[(t^2+z^2)^{1/2}]t\,dt\ . \tag{14}$$

In other cases the anisotropic terms in Eq. (4) are evaluated by direct space lattice summation. For $G\neq 0$, these coefficients are (approximately) exponentially decreasing functions of z, as seen in Fig. 2 along with $V_0(z)$.

In Fig. 3 we can see the contributions of various terms to $V_0(z)$. The MgO term is of order 20% of the well depth, while the three-body terms are of order a few percent. This hierarchy is rather typical of adlayer problems.[12–15] In Figs. 4 and 5 the corrugation is presented in terms of values of V above various symmetry positions

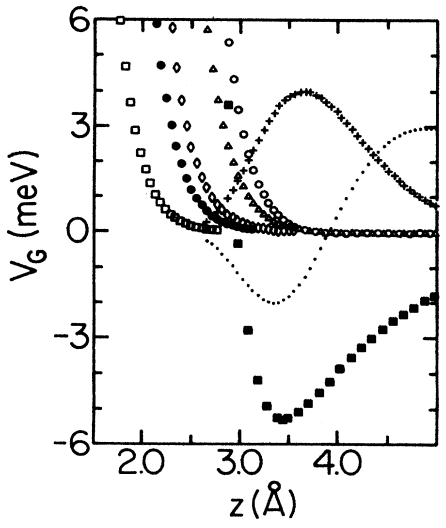

FIG. 2. Laterally averaged total potential $V_0(z)$ (solid squares) is presented along with five different Fourier components, $V_{G1}-V_{G5}$ [as in Eq. (16); open circles, open triangles, open diamonds, solid circles, and open squares, respectively]. The ground state (plusses) and the first excited state (dotted curve) wave functions are also shown. The results apply to the free-rotor case.

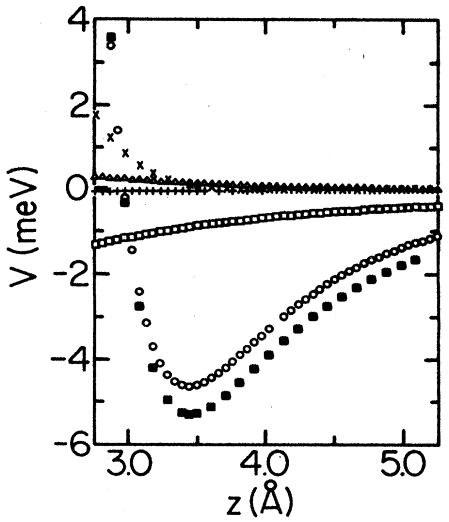

FIG. 3. Various contributions to the net laterally averaged potential $V_0(z)$ (solid squares) of a He atom above a CH_4 layer on MgO. Curves are V_a (open circles), V_s (open squares), V_3^{a-a} (open triangles), V_3^{a-s} (plusses), and V_t (crosses). This is the free-rotor case.

of the He atom. The peak-to-trough corrugation at zero energy is about 1.6 Å.

Energy eigenvalues and matrix elements of the Fourier components of the potential can be determined by solving the one-dimensional Schrödinger equation

$$-\frac{\hbar^2}{2m}\frac{d^2\Psi}{dz^2}+V_0(z)\Psi=\varepsilon\Psi\ . \tag{15}$$

The results for the eigenvalues appear in Table I for all orientations considered. The matrix elements of the Fourier components of the potential are given by

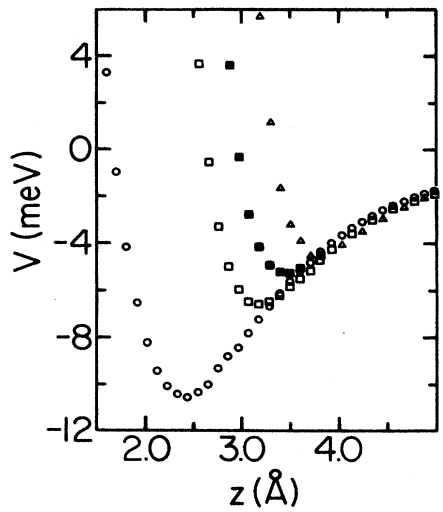

FIG. 4. Net potential experienced by a He atom above various symmetry positions: above the methane (triangles), bridge site (open squares), center (circles). Also shown in the laterally averaged potential (solid squares). This is the free-rotor case.

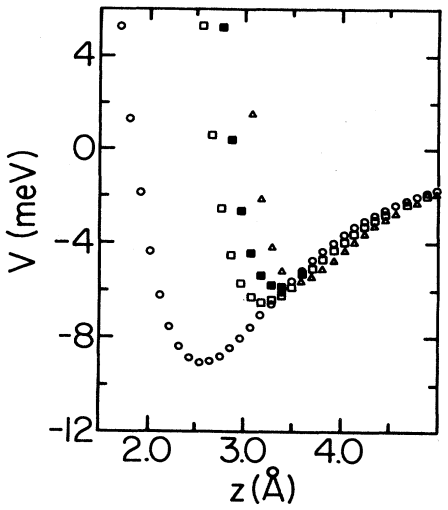

FIG. 5. Potential above various sites in the case of the dipod (011) CH_4 configuration shown in Fig. 1. The symbols are the same as in Fig. 4.

$$(n|V_G|n')\equiv\int dz\,\Psi_n(z)V_G(z)\Psi_{n'}(z)\ . \tag{16}$$

Table I gives also the results for some of the larger matrix elements for the free-rotor case. These results can be used, in principle, to determine the band structure of the He atoms on CH_4-plated surfaces. Near the ground state at $K=0$, the analysis is simplified,

$$E(\mathbf{K})=\varepsilon_0+\delta\varepsilon_0+\frac{\hbar^2K^2}{2m^*}\ , \tag{17}$$

where $\delta\varepsilon_0$ is the corrugation-induced shift of the ground state and m^* is the effective mass. If we use perturbation theory,

$$E(\mathbf{K})\approx\frac{\hbar^2k^2}{2m}\sum_{\substack{n,G\\(G\neq0)}}\frac{|(n|V_G|0)|^2}{\varepsilon_n-\varepsilon_0+(\hbar^2/2m)(G^2+2\mathbf{K}\cdot\mathbf{G})}\ . \tag{18}$$

Expanding for small K by including only the smallest nonzero wave vector $G_1\equiv|\mathbf{G}_{10}|=1.49$ Å^{-1},

$$\delta\varepsilon_0=-4\lambda M_1 \tag{19}$$

and

$$m^*=m(1-8\lambda^2)^{-1}\ , \tag{20}$$

where $M_1\equiv(0|V_{G1}|0)$ and the dimensionless expansion parameter

$$\lambda\equiv M_1\Big/\left[\frac{\hbar^2G_I^2}{2m}\right]\ . \tag{21}$$

For the free-rotor case, $M_1=0.31$ meV and $\lambda=0.27$, so that $\delta\varepsilon=-0.34$ meV and $m^*/m=2.4$. These are quite large values, consistent with the bumpiness of the potential apparent in Fig. 4.[31]

III. EXPERIMENTAL METHODS AND RESULTS

A. Methods

The experimental apparatus has been described before.[32] A highly monochromatic, liquid-nitrogen-temperature helium beam ($k=5.76$ Å, $\Delta k/k\approx1\%$) of narrow divergence ($\Delta\theta<10^{-3}$ rad) has a width of 0.6 mm at the sample. The sample holder allows polar and azimuthal rotation, as well as *in situ* cleaving, heating, and cooling of the MgO crystal. The scattered beams are detected by a quadrupole mass spectrometer with motion both in and out of the plane of incidence.

Temperature control and measurement are achieved by basically the same means as in the earlier Kr on graphite study.[12] Cooling is by a Displex (Air Products, Allentown, PA) closed-cycle refrigerator thermally linked to the sample plug by four copper braids, and the temperature may be set and regulated to within ±0.1 K by a temperature controller which drives a heater on the refrigerator cold tip. Additional heating is available from two lamp filaments contained within the sample plug. The sample plug temperature is measured by a calibrated platinum resistance thermometer using a three-wire connection. One wire grounded to the copper plug provides good thermal contact, while the other wires are heat sunk to the 77-K stage of the cold finger between thin sheets of mica.

TABLE I. Potential properties and eigenvalues, E_n, (all configurations) and matrix elements [Eq. (16)] (free rotor only) associated with the corrugation of the potential ($G_1=2\pi/a$, $G_2=\sqrt{2}G_1$). D and z_m are the well depth and minimum position, respectively. Energies are in meV and lengths are in angstroms.

	Theory				
	free rotor	dipod (010)	dipod (011)	tripod	Experiment
D	5.31	5.86	5.85	6.75	
z_m	3.44	3.39	3.39	3.18	
$\lvert E_0\rvert$	3.34	3.83	3.78	4.42	3.63±0.18
$\lvert E_1\rvert$	1.17	1.47	1.42	1.71	1.25±0.10
$\lvert E_2\rvert$	0.33	0.47	0.44	0.55	0.40±0.08
$\lvert E_3\rvert$	0.065	0.12	0.10	0.14	
$(0\lvert V_{G1}\rvert0)$	0.31				
$(1\lvert V_{G1}\rvert1)$	0.13				
$(0\lvert V_{G2}\rvert0)$	0.23				

The MgO single crystals ($5\times5\times25$ mm^3) were obtained from W. C. Spicer Ltd., London. Prior to deposition of the overlayer, the lamp filaments within the sample plug are briefly activated to bring the temperature to about 100 K. Then, as the temperature slowly falls, the crystal is cleaved, and the bare-surface quality is assessed before the CH_4 gas is dosed at temperatures around 50 K. The initial bare-surface reflection intensities were strong (typically 25% at an angle of incidence of 65°) and bound-state–resonance features were sharp, as in our previous room-temperature MgO work.[32] Oxygen heat treatment of the freshly cleaved surface was omitted so that the overlayer could be deposited without delay. Furthermore, only one deposition was made on each cleave, as specular intensities following layer desorption by heating up to 70 K (usually 3–4 h after deposition) were less than half the intensity following the cleave. Restoration of the surface by further heating was not a practical procedure due to the length of time involved in cooling back down, but was tried. It was found that more than 90% of the initial reflection intensity is restored at temperatures above 450 K. The time constant of the decay of the specular intensity from the methane layer was about 4 h. With the detector filament hot and the beam on, the pressure in the chamber was typically 3×10^{-10} Torr.

The major experimental errors in the selective adsorption line-shape measurements are caused by the uncertainties in the zeros of sample azimuthal and polar angles. The zero of the azimuthal angle normally can be determined from the symmetry point of the azimuthal scan of the specular intensity with an accuracy of a few tenths of a degree. The zero of the polar angle can be determined with the same accuracy by a lengthy series of adjustments prior to the experiment. As well as setting the polar angle zero, these adjustments assure that the crystal polar axis is collinear with the detector rotational axis and the incident beam is centered on it. Unfortunately, this method is not feasible in a low-temperature physisorption experiment since the freshly cleaved surface can be contaminated from the residual gases in the scattering chamber during the process of adjustment. Instead, a new method for determining corrections to the angle of incidence was used. Only the positions of specular and first-order peaks of the bare MgO(100) surface need be measured, and these can be done even after the physisorption measurements.

B. Deposition of CH_4 gas on MgO(001) surface

The methane film is grown by admitting research-grade CH_4 gas (99.99% purity) through a UHV leak valve via a stainless steel capillary aimed directly at the crystal from a distance of about 8 mm. The effective methane pressure near the crystal is roughly 30 times the pressure change measured by an ion gauge in the scattering chamber, according to estimates based either on the effusive flow of the gas from the dose tube,[33] or on the initial decay rate of the specular beam during dosing at a low temperature (≈30 K).

Typical dosing procedure starts with the freshly cleaved crystal still above 50 K. The leak valve is opened to allow a background pressure rise of about 0.2×10^{-10} Torr, and the specular reflection intensity is monitored over time as the temperature fulls at a rate of 0.6 K/min (Fig. 6). Under these conditions, monolayer growth begins at around 48 K and the specular intensity begins to decrease. After about 15 min the first layer is completed and the specular intensity reaches a plateau. At an angle of incidence of 65°, the observed specular reflection intensity is about 3% of that from the bare MgO surface.

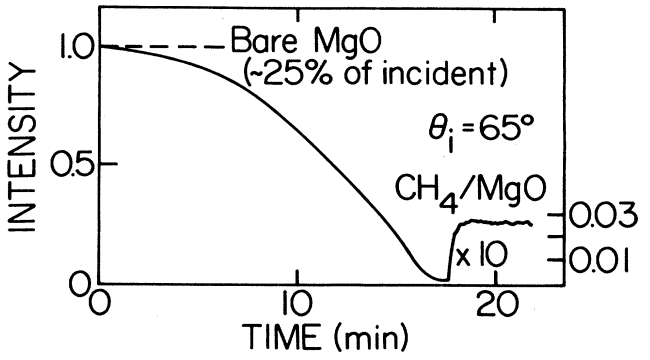

FIG. 6. Attenuation of He specular intensity as CH_4 is adsorbed at a constant rate of impingement. The surface temperature at $t=0$ (min) was about 52 K, and was lowered at a rate of approximately 0.6 K/min.

After monolayer completion, the temperature is allowed to fall further, usually to about 38 K where it is held constant, while the rate of impingement of methane gas is reduced or completely stopped to maintain the monolayer coverage.[34]

The lowest-order diffracted beam from monolayer CH_4 was observed along the bulk MgO(100) azimuth. Measurements at several angles of incidence between 65° and 80° yield a reciprocal lattice vector $|\mathbf{G}_{-10}|=1.50$ Å^{-1}. This confirms that monolayer CH_4 forms a commensurate $c(2\times2)$ phase in agreement with previous low-energy electron diffraction[3] (LEED) and neutron scattering measurements.[5,18] In addition to the $(\bar{1}0)$ diffracted beam, higher-order diffracted beams $(\bar{1}\bar{1})$ and $(\bar{2}0)$ of the $c(2\times2)$ phase were also observed.

C. Selective adsorption measurements

In the selective adsorption process, a He atom is trapped in a bound state of the surface attractive potential well for motion perpendicular to the surface, while being in a (2D) Bloch state for motion parallel to the surface. When this happens, a sudden change in the intensity of the specular beam as well as of various diffracted beams may be observed. This is because selective adsorption opens additional channels connecting the incident and diffracted beams. In the case that the parallel motion of the trapped He atom can be approximated by a 2D free particle state (i.e., at a nondegenerate resonance), the constraints of energy and parallel crystal momentum conservation yield the relation

$$\left[\frac{2m}{\hbar^2}\right]\varepsilon_n+(\mathbf{K}+\mathbf{G})^2=\mathbf{k}^2\ , \tag{22}$$

where $\mathbf{k}$ is the wave vector of the incident beam, $\mathbf{K}$ is the parallel part of $\mathbf{k}$ along the surface, $\mathbf{G}=(i,j)$ is a reciprocal lattice vector of the surface mesh, and ε_n is the (negative) energy of the nth bound-state solution of Eq. (15). Thus the bound state energies are deduced from the loci of selective adsorption resonances in $\mathbf{K}$ space, which should form circles of radii $[k_i^2-(2m/\hbar^2)\varepsilon_n]^{1/2}$ centered at $-\mathbf{G}=(-i,-j)$. The measurements were made by recording the He specular reflection intensity at a fixed polar incident angle θ while scanning the azimuthal angle ϕ.

Resonances were identified by first plotting all maxima and minima in $\mathbf{K}$ space, and then determining sets of circles and their respective reciprocal lattice vectors which gave consistent line shapes and energies. Figure 7 shows a sampling of these scans. Most of our data can be described by simple maximum or minimum resonances associated with energy levels $n=0$, 1, and 2, and with overlayer reciprocal-lattice vectors: (0,1), (0,2), and (0,−2). We believe we also observe the (1,−1) resonance, although it cannot be adequately described by either just a maximum or just a minimum line shape. The binding energies reported here are computed from the loci of resonances of (0,1), (0,2), and (0,−2) only. The resonance character (maximum or minimum), average energy, and energy standard deviation for each resonance $n(i,j)$ are given in Table II, along with labels which link each resonance to its respective line shape in Fig. 7. Figure 8 is a plot of the identified resonance positions in $\mathbf{K}$ space.

For clarity and definiteness, only the centers of maxima and minima were selected from the azimuthal scans for plotting. Then points which fell greatly off the circular loci were discarded, while many points which deviated slightly were included. Any features involving mixed line shapes (e.g., where resonances cross) were not used. Perturbations of selective adsorption line shape and position may be expected at circle crossings for a highly corrugated surface such as CH_4 on MgO, where the degeneracy of the resonant states will be lifted by relatively large matrix elements of the potential. These effects, plus broadening of resonance line shapes due to adlayer disorder, often prevented identification of resonances near the crossings. We were likewise unable to observe any splitting of resonance loci at the crossings. Evidence of resonances of higher-order reciprocal-lattice vectors such as (1,2) (labeled M in Fig. 7 and Table II), (−1,2), and (0,3) was also seen in some of the scans. These higher-order resonances are not plotted in Fig. 8 because the existence of these features is less certain. However the observation

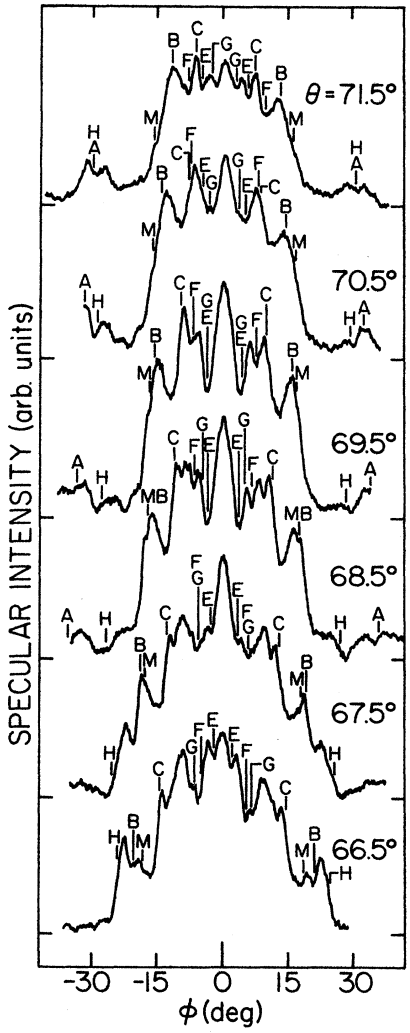

FIG. 7. A sampling of azimuthal scans of the He specular intensity from monolayer CH_4 on MgO at a temperature of 41 K. The curves are hand tracings of X-Y recorder charts. The capital letters label resonances as in Table II. The scale marks on the vertical axis are the zeros of the successive scans.

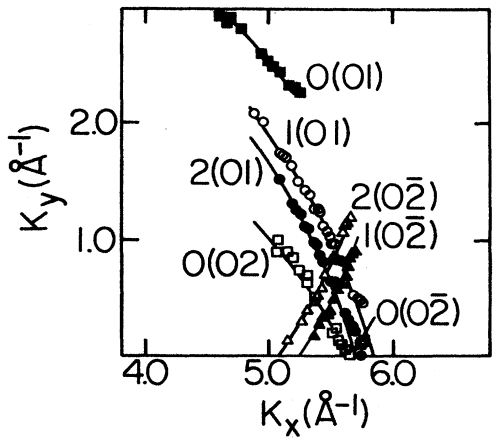

FIG. 8. Loci of selective-adsorption resonances $n(i,j)$ in the overlayer reciprocal space. The solid lines are circles centered at $-\mathbf{G}=(-i,-j)$ of radii corresponding to the average binding energies in Table I. The character and energy average of each resonance are found in Table II. For some resonances where the data were very closely spaced, some points have been omitted from the plot for clarity.

TABLE II. Selective-adsorption bound-state energies of ^{4}He-CH_4/MgO. The incident beam wave vector is 5.76 Å^{-1}.

Bound state n	G_{ij} i	j	Label[a]	Character	No. points	Energy (meV)
0	0	1	*A*	max	12	3.67±0.15
0	0	$\bar{2}$	*D*	min	4	3.62±0.13
0	0	2	*G*	min	16	3.61±0.21
0	1	$\bar{1}$	*H*	max-min[b]		
1	0	1	*B*	max	17	1.28±0.10
1	0	$\bar{2}$	*E*	min	29	1.22±0.09
2	0	1	*C*	max	20	0.43±0.07
2	0	$\bar{2}$	*F*	min	15	0.35±0.06
2	1	2	*M*	min		

[a]Indicates the position of the resonances as shown in Fig. 7.
[b]This resonance was found to be a minimum at lower angles of incidence and a maximum at higher angles of incidence.

of these resonances is consistent with the theoretical prediction of the relatively large corrugation (Fig. 2).

The selective-adsorption line shapes given in Table II are not in agreement with those expected from the rules of either Celli, Garcia, and Hutchison[35] or Wolfe and Weare.[36] Whenever we find minima, both rules predict maxima and vice versa. The assumptions upon which the rules are based, hard walls, elastic scattering, and small corrugation, are surely invalid for CH_4 on MgO, yet it is instructive to review the results for other systems.

Bare LiF,[37] NaF,[38] and MgO (Ref. 39) all follow these rules. Graphite follows the rules except for the (0,1) resonances.[40] This exception, in which predicted Wolfe-Weare maxima were observed to be minima, is attributed to inelastic effects.[41] The adlayer system Kr on graphite[12] showed minima in the place of rule-predicted maxima, while Xe on graphite[10,13] exhibited some cases of agreement and some of disagreement with both predictions of minima and of maxima. Another "soft" surface, Ag(110),[42] showed minima for the (0,1) resonances, in agreement with predictions.

However in the case of NaCl, the resonance line shapes are also opposite to those predicted by the rules.[43] Close-coupling calculations reproduced the experimental line shapes quite well.[44] Goodman and Vargas imply that adjustment of Δz, the real-space corrugation amplitude, enabled them to obtain "normal" line shapes for small Δz, and the experimental (anomalous) line shapes for large Δz. Their fitted value of the corrugation, 1.1 Å, and that of Hutson and Fowler, 1.05 Å, suggests that previous estimates [0.72 Å (Ref. 45)] may be low, and that corrugation *is* an important criterion for resonance line shape (compare with Ref. 39). Neither calculation employed an optical potential to simulate inelasticity, unlike the bare graphite resonance calculation.[41] The corrugation amplitude calculated here for He-CH_4/MgO scattering, 1.6 Å, and the observation of resonance line shapes opposite to those of the simple rules, strongly resemble the corresponding results for NaCl.

IV. COMPARISON OF BINDING ENERGIES

Average experimental binding energies and their standard deviations are given in Table I along with the calculated energies for the four molecular orientations [free rotor, dipod (010), dipod (011), and tripod] from Sec. II. Comparison between theory and experiment can only be made for the lowest three binding energies since the fourth binding energy was not resolved in the experiment.

For the ground state, the observed binding energy is 3.6±0.2 meV, which is in fair agreement with that of the free rotor and those of the two dipod configurations, but is substantially less than that of the tripod. For the first excited state, the observed binding energy agrees well with that for the free rotor and is at least 0.2 meV less than those for the other configurations. For the second excited state, the experimental value agrees equally well with those for the free rotor and the two dipods, and is 0.2 meV less than that for the tripod. The overall comparison indicates that theoretical calculations for the free rotor and dipolar configurations agree reasonably well with the experimental data.

The differences between theory and experiment may be due to error (from either part), or due to an actual orientational effect. For instance, a possible error in D of 0.3 meV due to the input parameters C_3 and z_a would mean a possible error of $\approx$0.3 meV in E_0 and leave either the free-rotor or dipod case in fair agreement with experiment, depending on the sign of the error. For the higher levels, the shifts would be smaller than 0.3 meV since the wave functions are more spread out. Further error in D might arise from uncertainty in the He-CH_4 pair potential.[19]

On the other hand, agreement could also be found if the orientational configuration of methane were intermediate to the free rotor and the dipods. There are several possible configurations which would satisfy this. One possibility is an ordered or disordered composite of free rotors and dipods. An analogous situation has been

predicted in a mean-field theory for the bulk CH_4 octahedral phase where one of the four molecules in each unit cell is in the free rotor state while the other three molecules all have preferred orientations.[46] Another possibility is that all methane molecules are in a single orientation which is intermediate to the free rotor and the two dipods. In both cases the resulting binding energies will lie somewhere between those of the free rotor and those of the dipods, and therefore fit the experimental data better.

Aside from their absolute accuracy, the calculated binding energies show relative differences between the different orientations which should be valid and which suggest that changes in the orientation of methane on MgO might be observable by selective adsorption. We expect the molecule to be in a free-rotor state at high temperature and to attain some degree of orientational order at low temperature, but we cannot predict at what temperature such a chance occurs. The small energy differences between the two dipod configurations indicate that the laterally averaged He-CH_4/MgO interaction potential is not very sensitive to the in-plane orientations of the methane molecule. The larger differences (greater than 0.5 meV for the ground state) between the dipods, the free rotor, and the tripod, however, suggest that changes in the out-of-plane orientation of methane on MgO should be revealed by shifts in experimental bound-state–resonance positions.

We looked for these shifts by making azimuthal scans at an angle of incidence of 70° down to our lowest temperature of 22 K. No shifts were found, indicating that any shift in the bound-state energies is less than 0.1 meV. According to the above discussion, we detect no change in the out-of-plane orientation of the methane molecules in this temperature range. This should be compared with the observation of hindrance of rotational motion for methane on graphite by NMR at 17 K (Ref. 47) and by inelastic neutron scattering at 30 K.[48] However, we do not exclude possible changes related to in-plane rotations in the same temperature range since the differences in calculated energies between the two dipod configurations are very small.

V. SUMMARY

Experimental and theoretical investigations have been made of the interaction and scattering of He near CH_4 adsorbed on MgO. The bound-state–resonance results are compatible with predictions based on either a free-rotor or dipod-oriented CH_4 layer. The line shapes do not conform to the "rules" derived from oversimplified models. Evidently theoretical calculations are in order. These are, however, difficult to perform if the substantial effects of inelasticity are included.

ACKNOWLEDGMENTS

The authors thank Professor Sam Fain for his helpful comments and acknowledge the National Science Foundation for their support of this work under Grant No. DMR-87-18771.

[1]J. P. Coulomb, T. S. Sullivan, and O. E. Vilches, Phys. Rev. B **30**, 4753 (1984).
[2]J. L. Jordan, J. P. McTague, J. B. Hastings, and L. Passell, Surf. Sci. **150**, L82 (1985).
[3]T. Meichel, J. Suzanne, and J.-M. Gay, C. R. Acad. Sci. (Paris) **303**, 989 (1986).
[4]T. Meichel, J. Suzanne, C. Girard, and C. Girardet, Phys. Rev. B **38**, 3781 (1988).
[5]J. P. Coulomb, K. Madih, B. Croset, and H. J. Lauter, Phys. Rev. Lett. **54**, 1536 (1985); M. Bienfait, J. M. Gay, and H. Blank, Surf. Sci. **204**, 331 (1988).
[6]J. Ma, D. L. Kingsbury, F.-C. Liu, and O. E. Vilches, Phys. Rev. Lett. **61**, 2348 (1989).
[7]B. Deprick and A. Julg, Nouveau J. Chim. **11**, 299 (1987).
[8]C. Girard and C. Girardet, Chem. Phys. Lett. **138**, 83 (1987).
[9]T. H. Ellis, G. Scoles, and U. Valbusa, Phys. Rev. B **24**, 2307 (1981); Chem. Phys. Lett. **94**, 247 (1983); H. Jonsson, J. H. Weare, T. H. Ellis, and G. Scoles, Surf. Sci. **180**, 353 (1987).
[10]G. Bracco, P. Cantini, E. Cavanna, R. Tatarek, and A. Glachant, Surf. Sci. **136**, 169 (1984).
[11]B. F. Mason, R. Caudano, and B. R. Williams, J. Chem. Phys. **77**, 562 (1982).
[12]J. Z. Larese, W. Y. Leung, D. R. Frankl, S. Chung, and M. W. Cole, Phys. Rev. Lett. **54**, 2533 (1985); S. Chung, A. Kara, J. Z. Larese, W. Y. Leung, and D. R. Frankl, Phys. Rev. B **35**, 4870 (1987).
[13]J. M. Hutson and C. Schwartz, J. Chem. Phys. **79**, 5179 (1983).
[14]S. Chung, N. Holter, and M. W. Cole, Phys. Rev. B **31**, 6660 (1985).
[15]C. Schwartz, Phys. Rev. B **34**, 2832 (1986).
[16]K. D. Gibson and S. J. Sibener, J. Chem. Phys. **88**, 7862 (1988).
[17]See the discussion by several individuals on pp. 57–65 of Faraday Discussions of the Chemical Society No. 80 (Royal Society of Chemistry, London, 1985).
[18]K. Madih, Ph.D. thesis, Universite D'Aix-Marseille, 1986.
[19]U. Buck, K. H. Kohl, A. Kohlhase, M. Faubel, and V. Staemmler, Mol. Phys. **55**, 1255 (1985).
[20]L. H. Hall, *Group Theory and Symmetry in Chemistry* (McGraw-Hill, New York, 1966), p. 199.
[21]K. Nath, Z. W. Gortel, and H. J. Kreuzer, Surf. Sci. **155**, 596 (1985); a somewhat lower value, $C_3 = 128$ meV, was obtained by S. Chung and M. W. Cole, Surf. Sci. **145**, 269 (1984) (using older optical data).
[22]We have taken the potential given for a dipod-orientation in Ref. 8 and, including anharmonicity, estimated the mean position z_a.
[23]B. Axilrod and E. Teller, J. Chem. Phys. **11**, 299 (1943); Y. Muto, Proc. Phys. Math. Soc. Jpn. **17**, 629 (1943).
[24]S. Rauber, J. R. Klein, M. W. Cole, and L. W. Bruch, Surf. Sci. **123**, 173 (1982).
[25]J. R. Klein and M. W. Cole, Surf. Sci. **134**, 722 (1983).
[26]J. R. Klein, L. W. Bruch, and M. W. Cole, Surf. Sci. **173**, 555 (1986).
[27]We have adjusted E_s and g_0 values to get the value $C_3 = 151$ meV Å^3 of Ref. 21.

[28]Results of Ref. 14 are generalized here [Eq. (12)] to include the corrugation effect, i.e., V_l depends on the x,y coordinates as well as z.

[29]$V_l(\mathbf{r})$ also depends on the orientation of the molecule, as shown in Eq. (12).

[30]W. A. Steele, *The Interaction of Gases with Solid Surfaces* (Pergamon, Oxford, 1984), Chap. 2.

[31]Note, however, that in the analogous problem of He interacting with gases on graphite or Ag, this truncated perturbation theory is unreliable. See C. Schwartz and M. W. Cole, Phys. Rev. B **34**, 1250 (1986).

[32]M. Mahgerefteh, D. R. Jung, and D. R. Frankl, Phys. Rev. B **39**, 3900 (1989).

[33]W. Y. Leung, Ph.D. thesis, The Penneylvania State University, 1985.

[34]Formation of a second layer has been observed at around 36 K by leaving the leak valve open and letting the temperature fall further. The specular intensity drops by a factor of 10 when the bilayer forms, and rises back to its monolayer level when the leak valve is closed and the second layer desorbs. Due to the weakness of the signal, no bound-state resonances could be observed.

[35]V. Celli, N. Carcia, and J. Hutchison, Surf. Sci. **87**, 112 (1979).

[36]K. L. Wolfe and J. H. Weare, Phys. Rev. Lett. **41**, 1663 (1978).

[37]D. A. Wesner and D. R. Frankl, Phys. Rev. B **24**, 1798 (1981).

[38]G. Derry, D. Wesner, S. V. Krishnaswamy, and D. R. Frankl, Surf. Sci. **74**, 245 (1978).

[39]D. R. Jung, M. Mahgerefteh, and D. R. Frankl, Phys. Rev. B **39**, 11 164 (1989) (see last two paragraphs).

[40]G. Derry, D. Wesner, W. Carlos, and D. R. Frankl, Surf. Sci. **87**, 629 (1979).

[41]K. L. Wolfe and J. H. Weare, Surf. Sci. **94**, 581 (1980).

[42]A. Luntz, L. Mattera, M. Rocca, F. Tommasini, and U. Valbusa, Surf. Sci. **120**, L447 (1982).

[43]W. Y. Leung, J. Z. Larese, and D. R. Frankl, Surf. Sci. **143**, L398 (1984).

[44]J. M. Hutson and P. W. Fowler, Surf. Sci. **173**, 337 (1986); F. O. Goodman and M. C. Vargas, *ibid.* **176**, 619 (1986).

[45]K. H. Rieder, Surf. Sci. **118**, 57 (1982).

[46]H. M. James and T. A. Keenan, J. Chem. Phys. **31**, 12 (1959).

[47]J. Z. Larese and R. J. Rollefson, Phys. Rev. B **31**, 3048 (1985).

[48]M. W. Newberry, T. Raymont, M. V. Smalley, R. K. Thomas, and J. W. White, Chem. Phys. Lett. **59**, 461 (1978); M. V. Smalley, A. Huller, R. K. Thomas, and J. W. White, Mol. Phys. **44**, 533 (1981).